# Rational approximation preconditioners for multiphysics problems

Ana Budiša $^{1*[0000-0003-1130-3309]},$ Xiaozhe Hu $^{2[0000-0001-7533-0416]},$ Miroslav Kuchta $^{1[0000-0002-3832-0988]},$ Kent-André Mardal $^{1,3[0000-0002-4946-1110]},$  and Ludmil Zikatanov $^{4[0000-0002-5189-4230]}$ 

- Simula Research Laboratory, 0164 Oslo, Norway \*ana@simula.no
  - <sup>2</sup> Tufts University, Medford, MA 02155, USA
    <sup>3</sup> University of Oslo, 0316 Oslo, Norway
- <sup>4</sup> Penn State University, University Park, PA 16802, USA

**Abstract.** We consider a class of mathematical models describing multiphysics phenomena interacting through interfaces. On such interfaces, the traces of the fields lie (approximately) in the range of a weighted sum of two fractional differential operators. We use a rational function approximation to precondition such operators. We first demonstrate the robustness of the approximation for ordinary functions given by weighted sums of fractional exponents. Additionally, we present more realistic examples utilizing the proposed preconditioning techniques in interface coupling between Darcy and Stokes equations.

**Keywords:** Rational approximation · Preconditioning · Multiphysics.

## 1 Introduction

Fractional operators arise in the context of preconditioning of coupled multiphysics systems and, in particular, in the problem formulations where the coupling constraint is enforced by a Lagrange multiplier defined on the interface. Examples include the so-called EMI equations in modeling of excitable tissue [30], reduced order models of microcirculation in 2d-1d [22,23] and 3d-1d [21,20] setting or Darcy/Biot-Stokes models [2,24]. We remark that fractional operators have been recently utilized also in monolithic solvers for formulations of Darcy/Biot-Stokes models without the Lagrange multipliers, see [6,5].

The coupling in the multiplier formulations is naturally posed in Sobolev spaces of fractional order. However, for parameter robustness of iterative methods, a more precise setting must be considered, where the interface problem is posed in the intersection (space) of parameter-weighted fractional order Sobolev spaces [17]. Here the sums of fractional operators induce the natural inner product. In the examples mentioned earlier, however, the interface preconditioners were realized by eigenvalue decomposition, and thus, while being parameter robust, the resulting solvers do not scale with mesh size. Using Darcy–Stokes system as the canonical example, we aim to show that rational approximations are crucial for designing efficient preconditioners for multiphysics systems.

There have been numerous works on approximating/preconditioning problems such as  $\mathcal{D}^s u = f$ , e.g. [27,9,4]. The rational approximation (RA) approach has been advocated, and several techniques based on it were proposed by Hofreither in [16,15] (where also a Python implementation of Best Uniform Rational Approximation (BURA) for  $x^{\lambda}$  is found). Further rational approximations used in preconditioning can be found in [13,12]. An interesting approach, which always leads to real-valued poles and uses Padé approximations of suitably constructed time-dependent problems, is found in [11]. In our numerical tests, we use Adaptive Antoulas-Anderson (AAA) algorithm [26] which is a greedy strategy for locating the interpolation points and then using the barycentric representation of the rational interpolation to define a function that is close to the target. In short, for a given continuous function f, the AAA algorithm returns a rational function that approximates the best uniform rational approximation to f.

The rest of the paper is organized as follows. In Section 2, we introduce a model problem that leads to the sum of fractional powers of a differential operator on an interface acting on weighted Sobolev spaces. In Section 3, we introduce the finite element discretizations that we employ for the numerical solution of such problems. Next, Section 4 presents some details on the rational approximation and the scaling of the discrete operators. In Section 5, we test several relevant scenarios and show the robustness of the rational approximation as well as the efficacy of the preconditioners. Conclusions are drawn in Section 6.

# 2 Darcy-Stokes model

We study interaction between a porous medium occupying  $\Omega_D \subset \mathbb{R}^d$ , d=2,3 surrounded by a free flow domain  $\Omega_S \supset \Omega_D$  given by a Darcy–Stokes model [24] as: For given volumetric source terms  $f_S: \Omega_S \to \mathbb{R}^d$  and  $f_D: \Omega_D \to \mathbb{R}$  find the Stokes velocity and pressure  $u_S: \Omega_S \to \mathbb{R}^d$ ,  $p_S: \Omega_S \to \mathbb{R}$  and the Darcy flux and pressure  $u_D: \Omega_D \to \mathbb{R}^d$ ,  $p_D: \Omega_D \to \mathbb{R}$  such that

$$-\nabla \cdot \sigma(u_S, p_S) = f_S \text{ and } \nabla \cdot u_S = 0 \quad \text{in } \Omega_S,$$

$$u_D + K\mu^{-1}\nabla p_D = 0 \text{ and } \nabla \cdot u_D = f_D \quad \text{in } \Omega_D,$$

$$u_S \cdot \nu_s + u_D \cdot \nu_D = 0 \quad \text{on } \Gamma,$$

$$-\nu_S \cdot \sigma(u_S, p_s) \cdot \nu_S - p_D = 0 \quad \text{on } \Gamma,$$

$$-P_{\nu_S} \left(\sigma(u_S, p_S) \cdot \nu_S\right) - \alpha \mu K^{-1/2} P_{\nu_S} u_S = 0 \quad \text{on } \Gamma.$$

$$(1)$$

Here,  $\sigma(u,p):=2\mu\epsilon(u)-pI$  with  $\epsilon(u):=\frac{1}{2}(\nabla u+\nabla u^T)$ . Moreover,  $\Gamma:=\partial\Omega_D\cap\partial\Omega_S$  is the common interface,  $\nu_S$  and  $\nu_D=-\nu_S$  represent the outward unit normal vectors on  $\partial\Omega_S$  and  $\partial\Omega_D$ . Given a surface with normal vector  $\nu$ ,  $P_{\nu}:=I-\nu\otimes\nu$  denotes a projection to the tangential plane with normal  $\nu$ . The final three equations in (1) represent the coupling conditions on  $\Gamma$ . Parameters of the model (which we shall assume to be constant) are viscosity  $\mu>0$ , permeability K>0 and Beavers-Joseph-Saffman parameter  $\alpha>0$ .

Finally, let us decompose the outer boundary  $\partial \Omega_S \setminus \Gamma = \Gamma_u \cup \Gamma_\sigma$ ,  $|\Gamma_i| > 0$ ,  $i = u, \sigma$  and introduce the boundary conditions to close the system (1)

$$u_S \cdot \nu_S = 0$$
 and  $P_{\nu_S} (\sigma(u_S, p_S) \cdot \nu_S) = 0$  on  $\Gamma_u$ ,  
 $\sigma(u_S, p_S) \cdot \nu_S = 0$  on  $\Gamma_\sigma$ .

Thus,  $\Gamma_u$  is an impermeable free-slip boundary. We remark that other conditions, in particular no-slip on  $\Gamma_u$ , could be considered without introducing additional challenges. However, unlike the tangential component, constraints for the normal component of velocity are easy<sup>5</sup> to implement in H(div)-conforming discretization schemes considered below.

Letting  $V_S \subset H_1(\Omega_S)$ ,  $V_D \subset H(\text{div}, \Omega_D)$ ,  $Q_S \subset L^2(\Omega_S)$ ,  $Q_D \subset L^2(\Omega_D)$  and  $Q \subset H^{1/2}(\Gamma)$  the variational formulation of (1) seeks to find  $w := (u, p, \lambda) \in W$ ,  $W := V \times Q \times \Lambda$ ,  $V := V_S \times V_D$ ,  $Q := Q_S \times Q_D$  and  $u := (u_S, u_D)$ ,  $p := (p_S, p_D)$  such that Aw = L in W', the dual space of W, where L is the linear functional of the right-hand sides in (1) and the problem operator A satisfies

$$\langle \mathcal{A}w, \delta w \rangle = a_S(u_S, v_S) + a_D(u_D, v_D) + b(u, q) + b_\Gamma(v, \lambda) + b(v, p) + b_\Gamma(u, \delta \lambda), \tag{2}$$

where  $\delta w := (v, q, \delta \lambda)$ ,  $v := (v_S, v_D)$ ,  $q := (q_S, q_D)$  and  $\langle \cdot, \cdot \rangle$  denotes a duality pairing between W and W'. The bilinear forms in (2) are defined as

$$a_{S}(u_{S}, v_{S}) := \int_{\Omega_{S}} 2\mu \epsilon(u_{S}) : \epsilon(v_{S}) \, \mathrm{d}x + \int_{\Gamma} \alpha \mu K^{-1/2} P_{\nu_{S}} u_{S} \cdot P_{\nu_{S}} v_{S} \, \mathrm{d}x,$$

$$a_{D}(u_{D}, v_{D}) := \int_{\Omega_{D}} \mu K^{-1} u_{D} \cdot v_{D} \, \mathrm{d}x,$$

$$b(v, p) := -\int_{\Omega_{S}} p_{S} \nabla \cdot v_{S} \, \mathrm{d}x - \int_{\Omega_{D}} p_{D} \nabla \cdot v_{D} \, \mathrm{d}x,$$

$$b_{\Gamma}(v, \lambda) := \int_{\Gamma} (v_{S} \cdot \nu_{S} + v_{D} \cdot \nu_{D}) \lambda \, \mathrm{d}s.$$

$$(3)$$

Here,  $\lambda$  represents a Lagrange multiplier whose physical meaning is related to the normal component of the traction vector on  $\Gamma$ ,  $\lambda := -\nu_S \cdot \sigma(u_S, p_S) \cdot \nu_S$ , see [24] where also well-posedness of the problem in the space W above is established.

Following [17], parameter-robust preconditioners for Darcy–Stokes operator  $\mathcal{A}$  utilize weighted sums of fractional operators on the interface. Specifically, as in our setting  $\Gamma$  is a closed surface, we shall consider the following operator

$$S := \mu^{-1}(-\Delta_{\Gamma} + I_{\Gamma})^{-1/2} + K\mu^{-1}(-\Delta_{\Gamma} + I_{\Gamma})^{1/2},\tag{4}$$

where we have used the subscript  $\Gamma$  to emphasize that the operators are considered on the interface. Letting  $A_S$  be the operator induced by the bilinear form

<sup>&</sup>lt;sup>5</sup> Conditions on the normal component can be implemented as Dirichlet boundary conditions and enforced by the constructions of the finite element trial and test spaces. The tangential component can be controlled e.g., by the Nitsche method [29] which modifies the discrete problem operator.

 $a_S$  in (3) we in turn define the Darcy-Stokes preconditioner as follows.

$$\mathcal{B} := \operatorname{diag} (A_S, \mu K^{-1}(I - \nabla \nabla \cdot), \mu^{-1}I, K\mu^{-1}I, S)^{-1}.$$
 (5)

Note that the operators I in the pressure blocks of the preconditioner act on different spaces/spatial domains, i.e.,  $Q_S$  and  $Q_D$ . We remark that in the context of Darcy–Stokes preconditioning, [14] consider BURA approximation for a simpler interfacial operator, namely,  $K\mu^{-1}(-\Delta_{\Gamma}+I_{\Gamma})^{1/2}$ . However, the preconditioner cannot yield parameter robustness, cf. [17].

#### 3 Mixed Finite Element Discretization

In order to assess numerically the performance of rational approximation of  $S^{-1}$  in (5), stable discretization of the Darcy–Stokes system is needed. In addition to parameter variations, here we also wish to show the algorithm's robustness to discretization and, in particular, the construction of the discrete multiplier space. To this end, we require a family of stable finite element discretizations.

Let  $k\geq 1$  denote the polynomial degree. For simplicity, to make sure that the Lagrange multiplier fits well with the discretization of both the Stokes and Darcy domain, we employ the same  $H(\operatorname{div})$  based discretization in both domains. That is, we discretize the Stokes velocity space  $V_S$  by Brezzi-Douglas-Marini  $\mathbb{BDM}_k$  elements [8] over simplicial triangulations  $\Omega^h_S$  of  $\Omega_S$  and likewise, approximations to  $V_D$  are constructed with  $\mathbb{BDM}_k$  elements on  $\Omega^h_D$ . Here, h denotes the characteristic mesh size. Note that by construction, the velocities and fluxes have continuous normal components across the *interior* facets of the respective triangulations. However, on the interface  $\Gamma$ , we do not impose any continuity between the vector fields. The pressure spaces  $Q_S$ ,  $Q_D$  shall be approximated in terms of discontinuous piecewise polynomials of degree k-1,  $\mathbb{P}^{\mathrm{disc}}_{k-1}$ . Finally, the Lagrange multiplier space is constructed by  $\mathbb{P}^{\mathrm{disc}}_k$  elements on the triangulation  $\Gamma^h := \Gamma^h_S$ , with  $\Gamma^h_S$  being the trace mesh of  $\Omega^h_S$  on  $\Gamma$ . For simplicity, we assume  $\Gamma^h_D = \Gamma^h_S$ .

Approximation properties of the proposed discretization are demonstrated in Figure 1. It can be seen that all the quantities converge with order k (or better) in their respective norms. This is particularly the case for the Stokes velocity, where the error is measured in the  $H^1$  norm.

Let us make a few remarks about our discretization. First, observe that by using BDM elements on a global mesh  $\Omega_S^h \cup \Omega_D^h$  the Darcy–Stokes problem (1) can also be discretized such that the mass conservation condition  $u_S \cdot \nu_S + u_D \cdot \nu_D = 0$  on  $\Gamma$  is enforced by construction, i.e. no Lagrange multiplier is required. Here, u is the global H(div)-conforming vector field, with  $u_i := u|_{\Omega_i}$ , i = S, D. Second, we note that the chosen discretization of  $V_S$  is only  $H(\text{div}, \Omega_S)$ -conforming. In turn, stabilization of the tangential component of the Stokes velocity is needed,

see, e.g., [3], which translates to modification of the bilinear form  $a_S$  in (3) as

$$a_{S}^{h}(u,v) := a_{S}(u,v) - \sum_{e \in F_{S}^{h}} \int_{e} 2\mu \{\!\{ \epsilon(u) \}\!\} \cdot [\![P_{\nu_{e}}v]\!] \, \mathrm{d}s$$

$$- \sum_{e \in F_{S}^{h}} \int_{e} 2\mu \{\!\{ \epsilon(v) \}\!\} \cdot [\![P_{\nu_{e}}u]\!] \, \mathrm{d}s + \sum_{e \in F_{S}^{h}} \int_{e} \frac{2\mu\gamma}{h_{e}} [\![P_{\nu_{e}}u]\!] \cdot [\![P_{\nu_{e}}v]\!] \, \mathrm{d}s,$$

$$(6)$$

see [18]. Here,  $F_S^h = F(\Omega_S^h)$  is the collection of interior facets e of triangulation  $\Omega_S^h$ , while  $\nu_e$ ,  $h_e$  denote respectively the facet normal and facet diameter. The stabilization parameter  $\gamma > 0$  has to be chosen large enough to ensure the coercivity of  $a_S^h$ . However, the value depends on the polynomial degree. Finally, for interior facet e shared by elements  $T^+$ ,  $T^-$  we define the (facet) jump of a vector v as  $[\![v]\!] := v|_{T^+\cap e} - v|_{T^-\cap e}$  and the (facet) average of a tensor  $\epsilon$  as  $[\![\epsilon]\!] := \frac{1}{2} (v|_{T^+\cap e} \cdot \nu_e + v|_{T^-\cap e} \cdot \nu_e)$ .

We conclude this section by discussing discretization of the operator  $(-\Delta+I)$  needed for realizing the interface preconditioner (4). Since, in our case, the multiplier space  $\Lambda_h$  is only  $L^2$ -conforming we adopt the symmetric interior penalty approach [10] so that in turn for  $u, v \in \Lambda_h$ ,

$$\langle (-\Delta + I)u, v \rangle := \int_{\Gamma} (\nabla u \cdot \nabla v + uv) \, \mathrm{d}x - \sum_{e \in F(\Gamma_h)} \int_{e} \{\!\!\{ \nabla u \}\!\!\} \, [\!\![v]\!\!] \, \mathrm{d}s$$

$$- \sum_{e \in F(\Gamma_h)} \int_{e} \{\!\!\{ \nabla v \}\!\!\} \, [\!\![u]\!\!] \, \mathrm{d}s + \sum_{e \in F(\Gamma_h)} \int_{e} \frac{\gamma}{h_e} [\!\![u]\!\!] [\!\![v]\!\!] \, \mathrm{d}s.$$

$$(7)$$

Here, the jump of a scalar f is computed as  $[\![f]\!] := f|_{T^+ \cap e} - f|_{T^- \cap e}$  and the average of a vector v reads  $\{\![v]\!] := \frac{1}{2} \left(v|_{T^+ \cap e} \cdot \nu_e + v|_{T^- \cap e} \cdot \nu_e\right)$ . As before,  $\gamma > 0$  is a suitable stabilization parameter.

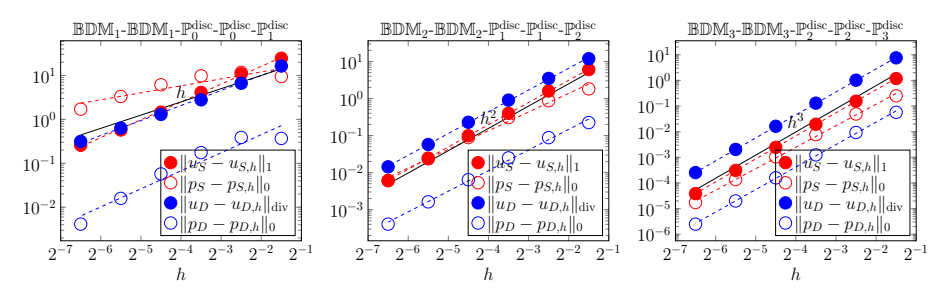


**Fig. 1.** Approximation properties of  $\mathbb{BDM}_k$ - $\mathbb{BDM}_k$ - $\mathbb{P}_{k-1}^{\mathrm{disc}}$ - $\mathbb{P}_k^{\mathrm{disc}}$ -discretization of the Darcy–Stokes problem. Two-dimensional setting is considered with  $\Omega_S=(0,1)^2$  and  $\Omega_D=(\frac{1}{4},\frac{3}{4})^2$ . Parameter values are set as K=2,  $\mu=3$  and  $\alpha=\frac{1}{2}$ . Left figure is for k=1 while k=2,3 is shown in the middle and right figures, respectively.

# 4 Rational approximation for the general problems of sums of fractional operators

Let  $s, t \in [-1, 1]$  and  $\alpha, \beta \ge 0$  where at least one of  $\alpha, \beta$  is not zero. For interval  $I \subset \mathbb{R}^+$ , consider a function

$$f(x) = (\alpha x^s + \beta x^t)^{-1}, \quad x \in I.$$

The basic idea is to find a rational function to approximate f on I, that is

$$f(x) \approx R(x) = \frac{P_{k'}(x)}{Q_k(x)},$$

where  $P_{k'}$  and  $Q_k$  are polynomials of degree k' and k, respectively. Assuming  $k' \leq k$ , the rational function can be given in the following partial fraction form

$$R(x) = c_0 + \sum_{i=1}^{N} \frac{c_i}{x - p_i},$$

for  $c_0 \in \mathbb{R}$ ,  $c_i, p_i \in \mathbb{C}$ , i = 1, 2, ..., N. The coefficients  $p_i$  and  $c_i$  are called *poles* and *residues* of the rational approximation, respectively.

We note that the rational approximation has been predominantly explored to approximate functions with only one fractional power, that is  $x^{-\bar{s}}$  for  $\bar{s} \in (0,1)$  and x>0. Additionally, the choice of the rational approximation method that computes the poles and residues is not unique. One possibility is the BURA method which first computes the best uniform rational approximation  $\bar{r}_{\beta}(x)$  of  $x^{\beta-\bar{s}}$  for a positive integer  $\beta>\bar{s}$  and then uses  $\bar{r}(x)=\frac{\bar{r}_{\beta}(x)}{x}$  to approximate  $x^{-\bar{s}}$ . Another possible choice is to use the rational interpolation of  $z^{-\bar{s}}$  to obtain  $\bar{r}(x)$ . The AAA algorithm proposed in [26] is a good candidate. The AAA method is based on the representation of the rational approximation in barycentric form and greedy selection of the interpolation points. Both approaches lead to the poles  $p_i \in \mathbb{R}$ ,  $p_i \leq 0$  for the case of one fractional power. An overview of rational approximation methods can be found in [15].

The location of the poles is crucial in rational approximation preconditioning. For  $\bar{f}(x) = x^{\bar{s}}$ ,  $\bar{s} \in (0,1)$  the poles of the rational approximation for  $\bar{f}$  are all real and negative. Hence, in the case of a positive definite operator  $\mathcal{D}$ , the approximation of  $\mathcal{D}^{\bar{s}}$  requires only inversion of positive definite operators of the form  $\mathcal{D} + |p_i|I$ , for  $i = 1, 2, \ldots, N$ ,  $p_i \neq 0$ . Such a result for rational approximation of  $\bar{f}$  with  $\bar{s} \in (-1,1)$  is found in a paper by H. Stahl [28]. In the following, we present an extensive set of numerical tests for the class of sum of fractional operators, which gives a wide class of efficient preconditioners for the multiphysics problems coupled through an interface. The numerical tests show that the poles remain real and nonpositive in most combinations of fractional exponents s and t.

Let V be a Hilbert space and V' be its dual. Consider a symmetric positive definite (SPD) operator  $A: V \to V'$ . Then, the rational function  $R(\cdot)$  can be

used to approximate f(A) as follows,

$$z = f(A)r \approx c_0 r + \sum_{i=1}^{N} c_i (A - p_i I)^{-1} r$$

with  $z \in V$  and  $r \in V'$ . The overall algorithm is shown in Algorithm 1.

**Algorithm 1** Compute z = f(A)r using rational approximation.

- 1: Solve for  $w_i$ :  $(A p_i I) w_i = r$ , i = 1, 2, ..., N.
- 2: Compute:  $z = c_0 r + \sum_{i=1}^{N} c_i w_i$

In our case, the operator A is a discretization of the Laplacian operator  $-\Delta$ , and I is the identity defined using the standard  $L^2$  inner product. Therefore, the equations in Step 1 of Algorithm 1 can be viewed as discretizations of the shifted Laplacian problems  $-\Delta w_i - p_i w_i = r$ ,  $p_i < 0$ , and we can use efficient numerical methods, such as Algebraic MultiGrid (AMG) methods [7,32], for their solution.

We would like to point out that in the implementation, the operators involved in Algorithm 1 are replaced by their matrix representations on a concrete basis and are properly scaled. We address this in more detail in the following section.

#### 4.1 Preconditioning

Let A be the stiffness matrix associated with  $-\Delta$  and M a corresponding mass matrix of the  $L^2$  inner product. Also, denote with  $n_c$  the number of columns of A. The problem we are interested in is constructing an efficient preconditioner for the solution of the linear system F(A)x = b. Thus, we would like to approximate  $f(A) = F(A)^{-1}$  using the rational approximation R(x) of  $f(x) = \frac{1}{F(x)}$ .

Let I be a  $n_c \times n_c$  identity matrix and let U be an M-orthogonal matrix of the eigenvectors of the generalized eigenvalue problem  $\mathsf{Au}_j = \lambda_j \mathsf{Mu}_j, j = 1, 2, \ldots, n_c$ , namely,

$$AU = MU\Lambda, \quad U^TMU = I \implies U^TAU = \Lambda.$$
 (8)

For any continuous function  $G:[0,\rho]\to\mathbb{R}$  we define

$$G(A) := MUG(\Lambda)U^{T}M, \text{ i.e., } f(A) = MUf(\Lambda)U^{T}M.$$
 (9)

where  $\rho := \rho(M^{-1}A)$  is the spectral radius of the matrix  $M^{-1}A$ .

A simple consequence from the Chebyshev Alternation Theorem is that the residues/poles for the rational approximation of f(x) for  $x \in [0, \rho]$  are obtained by scaling the residues/poles of the rational approximation of  $g(y) = f(\rho y)$  for  $y \in [0, 1]$ . Indeed, we have,  $c_i(f) = \rho c_i(g)$ , and  $p_i(f) = \rho p_i(g)$ . Therefore, in the

implementation, we need an upper bound on  $\rho$  (M<sup>-1</sup>A). For  $\mathbb{P}_1$  finite elements, such a bound can be obtained following the arguments from [31],

$$\rho\left(\mathsf{M}^{-1}\mathsf{A}\right) \le \frac{1}{\lambda_{\min}\left(\mathsf{M}\right)} \|\mathsf{A}\|_{\infty} = d(d+1) \left\| \operatorname{diag}(\mathsf{M})^{-1} \right\|_{\infty} \|\mathsf{A}\|_{\infty} \tag{10}$$

with d the spatial dimension<sup>6</sup>.

**Proposition 1.** Let  $R_f(\cdot)$  be the rational approximation for the function  $f(\cdot)$  on  $[0,\rho]$ . Then for the stiffness matrix A and mass matrix M satisfying (8), we have

$$f(A) \approx R_f(A) = c_0 M^{-1} + \sum_{i=1}^{N} c_i (A - p_i M)^{-1}.$$
 (11)

*Proof.* The relations (8) imply that  $UU^T = M^{-1}$ , and therefore,

$$AU - p_iMU = MU(\Lambda - p_iI) \iff (A - p_iM)U = MU(\Lambda - p_iI).$$

This is equivalent to  $(\Lambda - p_i \mathsf{I})^{-1} \underbrace{\mathsf{U}^{-1} \mathsf{M}^{-1}}_{\mathsf{U}^T} = \mathsf{U}^{-1} (\mathsf{A} - p_i \mathsf{M})^{-1}$ . Hence,

$$(\Lambda - p_i I)^{-1} = U^{-1} (A - p_i M)^{-1} U^{-T}.$$

A straightforward substitution in (9) then shows (11).

In addition, to apply the rational approximation preconditioner, we need to compute the actions of  $\mathsf{M}^{-1}$  and each  $(\mathsf{A} - \rho p_i \mathsf{M})^{-1}$ . If  $p_i \in \mathbb{R}$ ,  $p_i \leq 0$ , this leads to solving a series of elliptic problems where the AMG methods are very efficient.

# 5 Numerical results

In this section, we present two sets of experiments: (1) on the robustness of the rational approximation with respect to the scaling parameters and the fractional exponents; and (2) on the efficacy of the preconditioned minimal residual (MinRes) method as a solver for Darcy–Stokes coupled model. We use the AAA algorithm [26] to construct a rational approximation. The discretization and solver tools are Python modules provided by FEniCS\_ii [19], cbc.block [25], and interfaced with the HAZmath library [1].

<sup>&</sup>lt;sup>6</sup> Such estimates can be carried out for Lagrange finite elements of any polynomial degree because the local mass matrices are of a special type: a constant matrix, which depends only on the dimension and the polynomial degree, times the volume of the element.

#### 5.1 Approximating the sum of two fractional exponents

In this example, we test the approximation power of the rational approximation computed by AAA algorithm regarding different fractional exponents s, t and parameters  $\alpha, \beta$ . That is, we study the number of poles N required to achieve

$$||f - R||_{\infty} = \max_{x \in [0,1]} \left| (\alpha x^s + \beta x^t)^{-1} - \left( c_0 + \sum_{i=1}^N \frac{c_i}{x - p_i} \right) \right| \le \epsilon_{\text{RA}},$$

for a fixed tolerance  $\epsilon_{\rm RA}=10^{-12}$ . In this case, we consider the fractional function f to be defined on the unit interval I=(0,1]. As we noted earlier, however, the approximation can be straightforwardly extended to any interval. We also consider the scaling regarding the magnitude of parameters  $\alpha$  and  $\beta$ . Specifically, in case when  $\alpha>\beta$ , we rescale the problem with  $\gamma_{\alpha}=\frac{\beta}{\alpha}<1$  and approximate

$$\widetilde{f}(x) = (x^s + \gamma_{\alpha} x^t)^{-1} \approx R_{\widetilde{f}}(x).$$

Then the rational approximation for the original function f is given as

$$f(x) \approx R(x) = \frac{1}{\alpha} R_{\widetilde{f}}(x).$$

Similar can be done in case when  $\beta > \alpha$ .

The results are summarized in Figure 2. To obtain different parameter ratios  $\gamma_{\alpha}$ , we take  $\alpha \in \{10^{-9}, 10^{-6}, 10^{-3}, 1\}$  and  $\beta \in \{10^{-10}, 10^{-6}, 10^{-2}, 10^2\}$ . Furthermore, we vary the fractional exponents  $s, t \in [-1, 1]$  with the step 0.2. We observe that the number of poles N remains relatively uniform with varying the exponents, except in generic cases when  $s, t = \{-1, 0, 1\}$ . For example, for the combination (s, t) = (1, 1), the function we are approximating is  $f(x) = \frac{1}{2x}$ , thus the rational approximation should return only one pole  $p_1 = 0$  and residues  $c_0 = 0, c_1 = \frac{1}{2}$ . We also observe that for the fixed tolerance of  $\epsilon_{\rm RA} = 10^{-12}$ , we obtain a maximum of 22 poles in all cases.

Additionally, we remark that in most test cases, we retain real and negative poles, which is a desirable property to apply the rational approximation as a positive definite preconditioner. However, depending on the choice of fractional exponents s,t and tolerance  $\epsilon_{\rm RA}$ , the algorithm can produce positive or a pair of complex conjugate poles. Nevertheless, these cases are rare, and the number and the values of those poles are small. Therefore numerically, we do not observe any significant influence on the rational approximation preconditioner. More concrete analytical results on the location of poles for sums of fractionalities are part of our future research.

#### 5.2 The Darcy-Stokes problem

In this section, we discuss the performance of RA approximation of  $S^{-1}$  in the Darcy–Stokes preconditioner (5). To this end, we consider  $\Omega_S = (0,1)^2$ ,  $\Omega_D = (\frac{1}{4}, \frac{3}{4})^2$  and fix the value of Beavers-Joseph-Saffman parameter  $\alpha = 1$ 

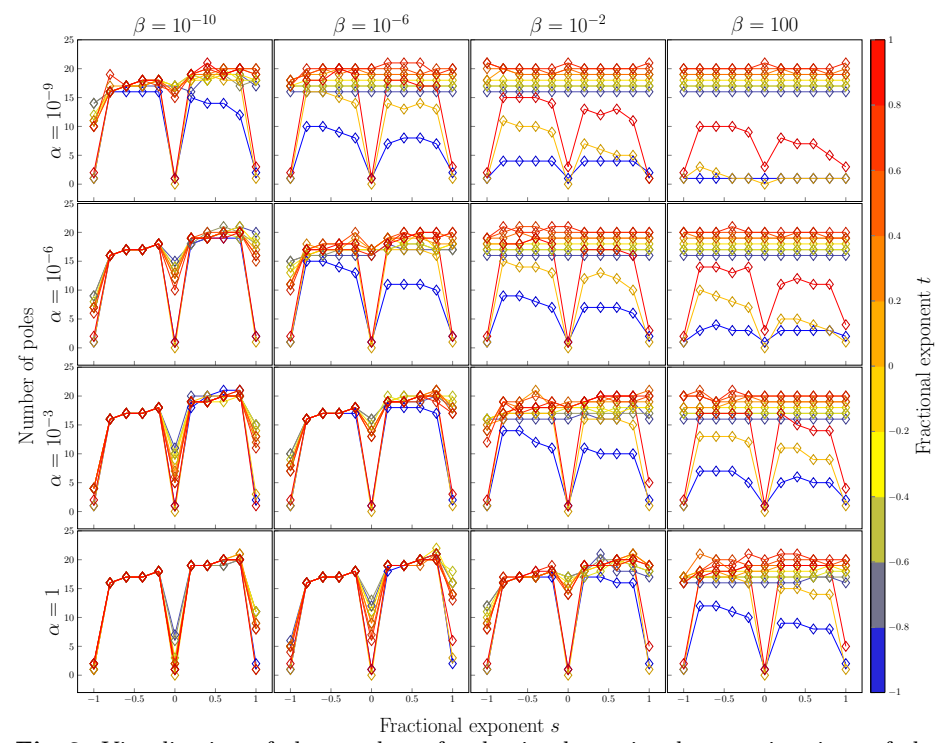


**Fig. 2.** Visualization of the number of poles in the rational approximations of the function  $f(x) = (\alpha x^s + \beta x^t)^{-1}$  for  $x \in (0,1]$  with regards to varying fractional exponents s,t and coefficients  $\alpha,\beta$ .

while permeability and viscosity are varied  $^7$   $10^{-6} \le K \le 1$  and  $10^{-6} \le \mu \le 10^2$ . The system is discretized by  $\mathbb{BDM}_k$ - $\mathbb{BDM}_k$ - $\mathbb{P}_{k-1}^{\mathrm{disc}}$ - $\mathbb{P}_{k-1}^{\mathrm{disc}}$ - $\mathbb{P}_k^{\mathrm{disc}}$  elements, k=1,2,3, which were shown to provide convergent approximations in Figure 1. A hierarchy of meshes  $\Omega_S^h$ ,  $\Omega_D^h$  is obtained by uniform refinement. We remark that the stabilization constants  $\gamma$  in (6) and (7) are chosen as  $\gamma=20k$  and  $\gamma=10k$  respectively. The resulting linear systems are then solved by preconditioned MinRes method. To focus on the RA algorithm in the preconditioner, for all but the multiplier block, an exact LU decomposition is used. Finally, the iterative solver is always started from a zero initial guess and terminates when the preconditioned residual norm drops below  $10^{-10}$ .

We present two sets of experiments. First, we fix the tolerance in the RA algorithm at  $\epsilon_{\rm RA}=2^{-40}\approx 10^{-12}$  and demonstrate that using RA in the preconditioner (5) leads to stable MinRes iterations for any practical values of the material parameters, the mesh resolution h and the polynomial degree k in the finite element discretization (see Figure 3). Here it can be seen that the number of iterations required for convergence is bounded in the above-listed quantities. Results for different polynomial degrees are largely similar and appear to be

<sup>&</sup>lt;sup>7</sup> These ranges are identified as relevant for many applications in biomechanics [6].

mostly controlled by material parameters. However, despite the values of K,  $\mu$  spanning several orders of magnitude, the iterations vary only between 30 to 100.

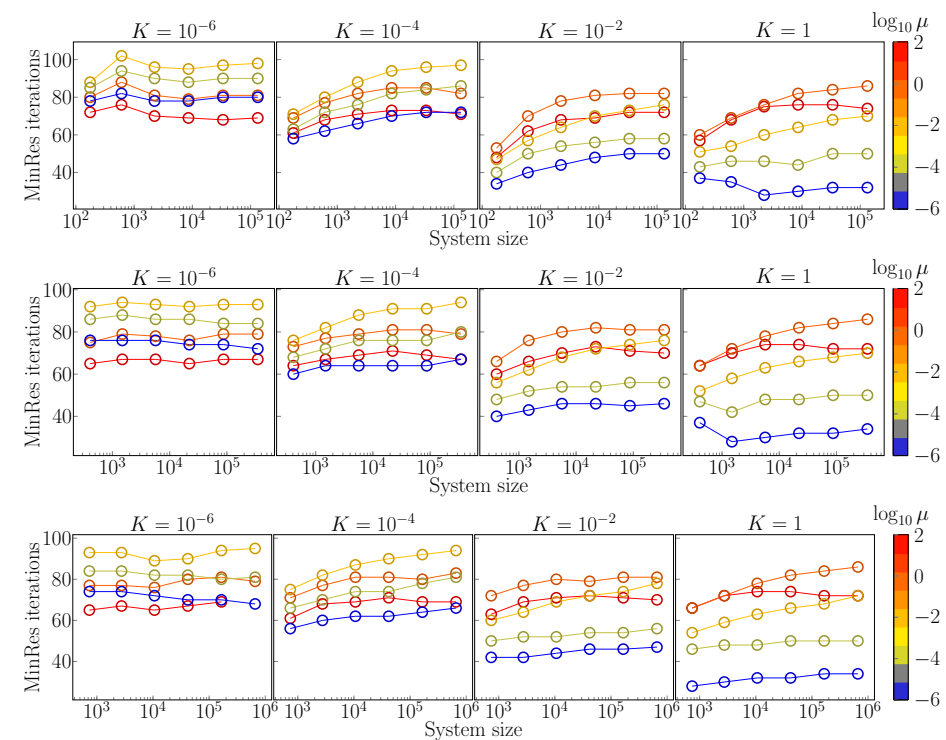


**Fig. 3.** Number of MinRes iterations required for convergence with preconditioner (5) using the RA with tolerance  $\epsilon_{\text{RA}} = 2^{-40}$ . Setup from Figure 1 is considered with the system discretized by  $\mathbb{BDM}_k$ - $\mathbb{BDM}_k$ - $\mathbb{P}_{k-1}^{\text{disc}}$ - $\mathbb{P}_{k-1}^{\text{disc}}$ - $\mathbb{P}_k^{\text{disc}}$  elements. (Top) k=1, (middle) k=2, (bottom) k=3.

Next, we assess the effects of the accuracy in RA on the performance of preconditioned MinRes solver. Let us fix k=1 and vary the material parameters as well as the RA tolerance  $\epsilon_{\rm RA}$ . In Figure 4, we observe that the effect of  $\epsilon_{\rm RA}$  varies with material properties (which enter the RA algorithm through scaling). In particular, it can be seen that for K=1, the number of MinRes iterations is practically constant for any  $\epsilon_{\rm RA} \leq 10^{-1}$ . On the other hand, when  $K=10^{-6}$ , the counts vary with  $\epsilon_{\rm RA}$  and to a lesser extent with  $\mu$ . Here, lower accuracy typically leads to a larger number of MinRes iterations. However, for  $\epsilon_{\rm RA} \leq 10^{-4}$  the iterations behave similarly. We remark that with  $K=10^{-6}$  (and any  $10^{-6} \leq \mu \leq 10^2$ ), the tolerance  $\epsilon_{\rm RA}=10^{-1}$  leads to 2 poles, cf. Figure 5, while for K=1 there are at least 5 poles needed in the RA approximation.

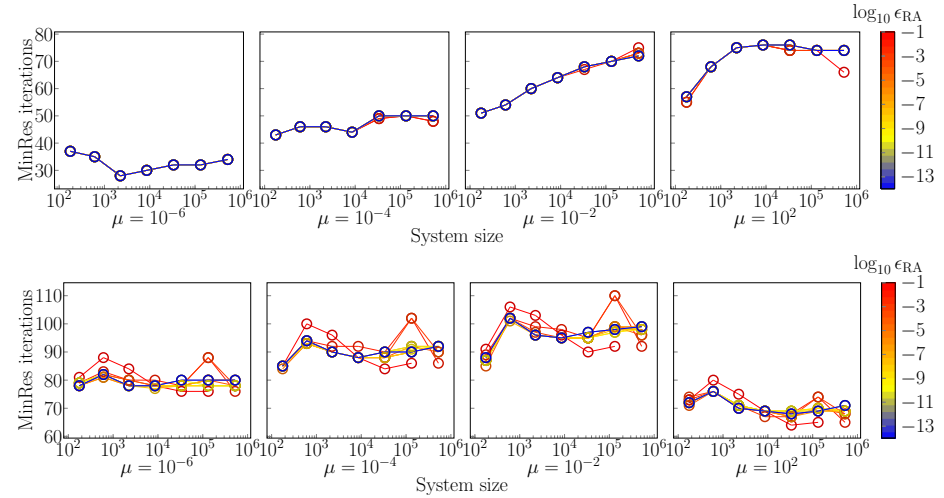


**Fig. 4.** Number of MinRes iterations required for convergence with preconditioner (5) using the RA with varying tolerance  $\epsilon_{\text{RA}}$ . (Top) K=1. (Bottom)  $K=10^{-6}$ . Setup as in Figure 3 is used with discretization by  $\mathbb{BDM}_1$ - $\mathbb{BDM}_1$ - $\mathbb{P}_0^{\text{disc}}$ - $\mathbb{P}_1^{\text{disc}}$ - $\mathbb{P}_1^{\text{disc}}$  elements.

Our results demonstrate that RA approximates  $S^{-1}$  in (4), which leads to a robust, mesh, and parameter-independent Darcy–Stokes solver. We remark that though the algorithm complexity is expected to scale with the number of degrees of freedom on the interface,  $n_h = \dim \Lambda_h$ , which is often considerably smaller than the total problem size, the setup cost may become prohibitive. This is particularly true for spectral realization, which often results in  $\mathcal{O}(n_h^3)$  complexity. To address such issues, we consider how the setup time of RA and the solution time of the MinRes solver depend on the problem size.

In Figure 5 we show the setup time of RA (for fixed material parameters) as function of mesh size and  $\epsilon_{\rm RA}$ . It can be seen that the times are  $< 0.1\,\mathrm{s}$  and practically constant with h (and  $n_h$ ). As with the number of poles, the small variations in the timings with h are likely due to different scaling of the matrices A and M. We note that in our experiments  $32 \le n_h \le 1024$ . Moreover, since  $\Lambda_h$  is in our experiments constructed from  $\mathbb{P}_1^{\mathrm{disc}}$  we apply the estimate (10).

In Figure 5, we finally plot the dependence of the solution time of the preconditioned MinRes solver on the problem size. Indeed we observe that the solver is of linear complexity. In particular, application of rational approximation of  $S^{-1}$  in our implementation requires  $\mathcal{O}(n_h)$  operations. We remark that here the solvers for the shifted Laplacian problems are realized by the conjugate gradient method with AMG as a preconditioner. Let us also recall that the remaining blocks of the preconditioner are realized by LU, where the setup cost is not included in our timings. However, LU does not define efficient preconditioners for the respective blocks. Here instead, multilevel methods could provide order optimality, and this is a topic of current and future research.

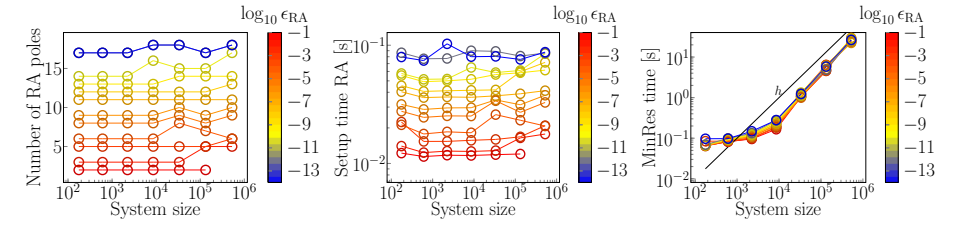


**Fig. 5.** Dependence of the number of poles (left), the setup time of RA (center) and runtime of the MinRes solver (right) on mesh size h and RA tolerance  $\epsilon_{\rm RA}$ . Parameters in the Darcy–Stokes problem are fixed at  $K=10^{-6}$ ,  $\mu=10^{-2}$  and  $\alpha=1$ . Setup as in Figure 3 is used with discretization by  $\mathbb{BDM}_1$ - $\mathbb{BDM}_1$ - $\mathbb{P}_0^{\rm disc}$ - $\mathbb{P}_0^{\rm disc}$ - $\mathbb{P}_1^{\rm disc}$  elements.

### 6 Conclusions

We have demonstrated that RA provides order optimal preconditioners for sums of fractional powers of SPD operators and can thus be utilized to construct parameter robust and order optimal preconditioners for multiphysics problems. The results are of practical interest for constructing efficient preconditioning on interfaces in models for which fractional weighted Sobolev spaces are the natural setting for the resulting differential operators, for example, when flow interacts with porous media. The techniques presented here could aid the numerical simulations in a wide range of biology, medicine, and engineering applications.

# 7 Acknowledgments

A. Budiša, M. Kuchta, K. A. Mardal, and L. Zikatanov acknowledge the financial support from the SciML project funded by the Norwegian Research Council grant 102155. The work of X. Hu is partially supported by the National Science Foundation under grant DMS-2208267. M. Kuchta acknowledges support from the Norwegian Research Council grant 303362. The work of L. Zikatanov is supported in part by the U. S.-Norway Fulbright Foundation and the U. S. National Science Foundation grant DMS-2208249.

# References

- 2. Ambartsumyan, I., Khattatov, E., Yotov, I., Zunino, P.: A Lagrange multiplier method for a Stokes-Biot fluid-poroelastic structure interaction model. Numerische Mathematik **140**(2), 513–553 (2018)
- 3. Ayuso, B., Brezzi, F., Marini, L.D., Xu, J., Zikatanov, L.: A simple preconditioner for a discontinuous Galerkin method for the Stokes problem. Journal of Scientific Computing **58**(3), 517–547 (2014)
- 4. Bonito, A., Pasciak, J.E.: Numerical approximation of fractional powers of elliptic operators. Math. Comp. 84(295), 2083–2110 (2015)

- Boon, W.M., Hornkjøl, M., Kuchta, M., Mardal, K.A., Ruiz-Baier, R.: Parameterrobust methods for the Biot-Stokes interfacial coupling without Lagrange multipliers. Journal of Computational Physics 467, 111464 (2022)
- Boon, W.M., Koch, T., Kuchta, M., Mardal, K.A.: Robust monolithic solvers for the Stokes-Darcy problem with the Darcy equation in primal form. SIAM Journal on Scientific Computing 44(4), B1148-B1174 (2022)
- 7. Brandt, A., McCormick, S.F., Ruge, J.W.: Algebraic multigrid (AMG) for automatic multigrid solutions with application to geodetic computations. Tech. rep., Inst. for Computational Studies, Fort Collins, CO (October 1982)
- Brezzi, F., Douglas, J., Marini, L.D.: Two families of mixed finite elements for second order elliptic problems. Numerische Mathematik 47(2), 217–235 (1985)
- Chen, L., Nochetto, R.H., Otárola, E., Salgado, A.J.: Multilevel methods for nonuniformly elliptic operators and fractional diffusion. Math. Comp. 85(302), 2583–2607 (2016)
- Di Pietro, D.A., Ern, A.: Mathematical aspects of discontinuous Galerkin methods, vol. 69. Springer Science & Business Media (2011)
- Duan, B., Lazarov, R.D., Pasciak, J.E.: Numerical approximation of fractional powers of elliptic operators. IMA J. Numer. Anal. 40(3), 1746–1771 (2020)
- Harizanov, S., Lazarov, R., Margenov, S., Marinov, P.: Numerical solution of fractional diffusion-reaction problems based on BURA. Comput. Math. Appl. 80(2), 316–331 (2020)
- Harizanov, S., Lazarov, R., Margenov, S., Marinov, P., Pasciak, J.: Analysis of numerical methods for spectral fractional elliptic equations based on the best uniform rational approximation. J. Comput. Phys. 408, 109285, 21 (2020)
- Harizanov, S., Lirkov, I., Margenov, S.: Rational approximations in robust preconditioning of multiphysics problems. Mathematics 10(5), 780 (2022)
- 15. Hofreither, C.: A unified view of some numerical methods for fractional diffusion. Computers & Mathematics with Applications 80(2), 332–350 (Jul 2020)
- 16. Hofreither, C.: An algorithm for best rational approximation based on barycentric rational interpolation. Numer. Algorithms 88(1), 365–388 (2021)
- 17. Holter, K.E., Kuchta, M., Mardal, K.A.: Robust preconditioning of monolithically coupled multiphysics problems. arXiv preprint arXiv:2001.05527 (2020)
- 18. Hong, Q., Kraus, J., Xu, J., Zikatanov, L.: A robust multigrid method for discontinuous Galerkin discretizations of Stokes and linear elasticity equations. Numerische Mathematik 132(1), 23–49 (2016)
- 19. Kuchta, M.: Assembly of multiscale linear PDE operators. In: Numerical Mathematics and Advanced Applications ENUMATH 2019, pp. 641–650. Springer (2021)
- 20. Kuchta, M., Laurino, F., Mardal, K.A., Zunino, P.: Analysis and approximation of mixed-dimensional PDEs on 3D-1D domains coupled with Lagrange multipliers. SIAM Journal on Numerical Analysis **59**(1), 558–582 (2021)
- 21. Kuchta, M., Mardal, K.A., Mortensen, M.: Preconditioning trace coupled 3d-1d systems using fractional Laplacian. Numerical Methods for Partial Differential Equations **35**(1), 375–393 (2019)
- 22. Kuchta, M., Nordaas, M., Verschaeve, J.C., Mortensen, M., Mardal, K.A.: Preconditioners for saddle point systems with trace constraints coupling 2d and 1d domains. SIAM Journal on Scientific Computing 38(6), B962–B987 (2016)
- 23. Lamichhane, B.P., Wohlmuth, B.I.: Mortar finite elements for interface problems. Computing **72**(3), 333–348 (2004)
- 24. Layton, W.J., Schieweck, F., Yotov, I.: Coupling fluid flow with porous media flow. SIAM Journal on Numerical Analysis **40**(6), 2195–2218 (2002)

- Mardal, K.A., Haga, J.B.: Block preconditioning of systems of PDEs. In: Automated solution of differential equations by the finite element method, pp. 643–655.
   Springer (2012)
- Nakatsukasa, Y., Sète, O., Trefethen, L.N.: The AAA Algorithm for Rational Approximation. SIAM Journal on Scientific Computing 40(3), A1494–A1522 (Jan 2018)
- Nochetto, R.H., Otárola, E., Salgado, A.J.: A PDE approach to space-time fractional parabolic problems. SIAM J. Numer. Anal. 54(2), 848–873 (2016)
- 28. Stahl, H.R.: Best uniform rational approximation of  $x^{\alpha}$  on [0, 1]. Acta Math. **190**(2), 241–306 (2003)
- 29. Stenberg, R.: On some techniques for approximating boundary conditions in the finite element method. Journal of Computational and applied Mathematics **63**(1-3), 139–148 (1995)
- 30. Tveito, A., Jæger, K.H., Kuchta, M., Mardal, K.A., Rognes, M.E.: A cell-based framework for numerical modeling of electrical conduction in cardiac tissue. Frontiers in Physics 5 (2017)
- 31. Wathen, A.J.: Realistic eigenvalue bounds for the Galerkin mass matrix. IMA Journal of Numerical Analysis **7**(4), 449–457 (1987)
- 32. Xu, J., Zikatanov, L.: Algebraic multigrid methods. Acta Numer. **26**, 591–721 (2017)